Available online at www.sciencedirect.com
ScienceDirect
Physics Letters B 657 (2007) 143–147
PHYSICS LETTERS B
www.elsevier.com/locate/physletb

Effects of a multi-quark interaction on color superconducting phase transition in an extended NJL model

Kouji Kashiwa [a], Masayuki Matsuzaki [b,*], Hiroaki Kouno [c], Masanobu Yahiro [a]

[a] *Department of Physics, Graduate School of Sciences, Kyushu University, Fukuoka 812-8581, Japan*
[b] *Department of Physics, Fukuoka University of Education, Munakata, Fukuoka 811-4192, Japan*
[c] *Department of Physics, Saga University, Saga 840-8502, Japan*

Received 21 May 2007; accepted 25 August 2007

Available online 6 September 2007

Editor: L. Alvarez-Gaumé

Abstract

We study the interplay of the chiral and the color superconducting phase transition in an extended Nambu–Jona-Lasinio model with a multi-quark interaction that produces the nonlinear chiral–diquark coupling. We observe that this nonlinear coupling adds up coherently with the ω^2 interaction to either produce the chiral–color superconductivity coexistence phase or cancel each other depending on its sign. We discuss that a large coexistence region in the phase diagram is consistent with the quark–diquark picture for the nucleon whereas its smallness is the prerequisite for the applicability of the Ginzburg–Landau approach.

PACS: 11.30.Rd; 12.40.-y

The findings of recent ultra-relativistic heavy ion collision experiments have stimulated a paradigm shift, that is, quark–gluon plasma (QGP) is not a weakly interacting near ideal gas but a strongly interacting near perfect fluid, called sQGP, at least slightly above the transition temperature [1–3]. Quantum chromodynamics (QCD) exhibits a variety of forms of matter also at high density; chiral symmetry restoration, deconfinement, and color superconductivity (CSC) [4]. As for CSC, various sub-phases at intermediate density are discussed recently in addition to standard two flavor superconductivity and color flavor locking.

First principle lattice QCD simulations describe high temperature phenomena but their applicability to finite density is limited due to the well-known sign problem and/or zero eigen values of the fermion matrix. Therefore effective models, such as the Nambu–Jona-Lasinio (NJL) model [5–8] or the random matrix model [9,10], must be employed. Recently the Polyakov–NJL model that handles not only chiral restoration but also deconfinement is actively studied [11–14].

Before CSC came into consideration, standard effective models predicted that chiral restoration at high density is a first order transition. (See also Ref. [15] and references cited therein that go beyond the mean field approximation.) However, the vector interaction, which is not forbidden from symmetry consideration, rather necessary from a view point of nuclear physics but often ignored, may change the situation [16,17]. The competition between the chiral $\langle\bar{q}q\rangle$ and the diquark $\langle qq\rangle$ condensates on the temperature–chemical potential $(T-\mu)$ plane was first considered by Berges and Rajagopal [18]. In their calculation, the two types of condensates are mutually exclusive. But, in principle, they can coexist, i.e., quarks dressing chiral condensate can pair up. Pairing between such constituent quarks would lead to the quark–diquark picture for the nucleon [19]. On the other hand, recently Hatsuda et al. obtained interesting results including a new end point induced by the U(1) anomaly in the three flavor case, using a model-independent Ginzburg–Landau (GL) approach to the $T-\mu$ phase diagram [20]. Here it should be noted that the GL

* Corresponding author.
E-mail address: matsuza@fukuoka-edu.ac.jp (M. Matsuzaki).

0370-2693/$ – see front matter
doi:10.1016/j.physletb.2007.08.071

approach is applicable when all the order parameters considered are small, since the free energy is expanded with respect to them. In the present case, both σ and Δ should be small. This situation is realized in the vicinity of each phase transition, if the coexistence region is small or vanishes. It is thus an important information how large the region is, and effective models are useful to answer the question.

We adopt a framework that can handle these aspects of the QCD phase diagram on the same footing—an extended NJL model with multi-quark interactions. (For introduction of multi-quark interactions, see also Osipov et al. [21,22] and Huguet et al. [23,24].) In a previous paper [25], we found that the $\sigma^2\omega^2$ and the σ^4 interactions sharpen the chiral transition weakened by the ω^2 interaction and also that the σ^4 interaction shifts the critical end point to a higher T, lower μ point. In the present Letter, we discuss the interplay of the chiral and the diquark condensates brought about by the $\sigma^2\Delta^2$ interaction and its coherence/competition with the ω^2 interaction. Here, σ, ω, and Δ denote the scalar, vector, and diquark auxiliary mean fields, respectively, defined later. Note that our study is limited to the two flavor case at present.

The Lagrangian density of the extended NJL model adopted in the present work is given by

$$\begin{aligned}\mathcal{L} = {}& \bar{q}(i\partial\!\!\!/ - m_0)q + \big[g_{2,0}\big((\bar{q}q)^2 + (\bar{q}i\gamma_5\vec{\tau}q)^2\big) \\ & + g_{4,0}\big((\bar{q}q)^2 + (\bar{q}i\gamma_5\vec{\tau}q)^2\big)^2 \\ & - g_{0,2}\big(\bar{q}\gamma^\mu q\big)^2 - g_{2,2}\big((\bar{q}q)^2 + (\bar{q}i\gamma_5\vec{\tau}q)^2\big)\big(\bar{q}\gamma^\mu q\big)^2 \\ & + d_{0,2}\big(\big(i\bar{q}^c\varepsilon\epsilon^b\gamma_5 q\big)\big(i\bar{q}\varepsilon\epsilon^b\gamma_5 q^c\big) \\ & + \big(i\bar{q}^c\varepsilon\epsilon^b\gamma_5 q\big)\big(i\bar{q}\varepsilon\epsilon^b\gamma_5 q^c\big)\big) \\ & + d_{2,2}(\bar{q}q)^2\big(\big(i\bar{q}^c\varepsilon\epsilon^b\gamma_5 q\big)\big(i\bar{q}\varepsilon\epsilon^b\gamma_5 q^c\big) \\ & + \big(i\bar{q}^c\varepsilon\epsilon^b\gamma_5 q\big)\big(i\bar{q}\varepsilon\epsilon^b\gamma_5 q^c\big)\big) + \cdots\big], \end{aligned} \tag{1}$$

where $q^c = C\bar{q}^T$ and $\bar{q}^c = q^T C$ are the charge-conjugation spinors, $C = i\gamma^2\gamma^0$ is the charge-conjugation matrix, q is the two flavor quark field, $\vec{\tau} = (\tau^1, \tau^2, \tau^3)$ are the Pauli matrices, $m_0 = \mathrm{diag}(m_u, m_d)$ is the current quark mass matrix, ε and ϵ^b are the totally antisymmetric tensors in the flavor and color spaces, and $g_{i,j}$ and $d_{m,n}$ $(i, j, m, n = 0, 1, 2, \ldots)$ are the coupling constants of quark–quark interactions. We consider only the four- and eight-quark interactions ignoring higher-order interactions denoted by ellipsis in the Lagrangian density. Among the physically important eight-quark interactions, $g_{4,0}$ and $g_{2,2}$ terms will be ignored in the following, since their roles have been clarified in our previous paper [25] as mentioned above and we would like to concentrate on the chiral–diquark coexistence. Under the standard mean field approximation (MFA), the Lagrangian density reads

$$\begin{aligned}\mathcal{L}_{\mathrm{MFA}} = {}& \bar{q}\big(i\partial\!\!\!/ - (m_0 + \Sigma_{\mathrm{s}}) + \Sigma_{\mathrm{v}}\gamma^0\big)q - \frac{1}{2}\Sigma_{\mathrm{d}}^{*b}\big(i\bar{q}^c\varepsilon\epsilon^b\gamma_5 q\big) \\ & - \frac{1}{2}\Sigma_{\mathrm{d}}^{b}\big(i\bar{q}\varepsilon\epsilon^b\gamma_5 q^c\big) - U, \end{aligned} \tag{2}$$

where

$$\begin{aligned}\Sigma_{\mathrm{s}} &= -2\big(g_{2,0}\sigma + d_{2,2}\sigma|\Delta|^2\big), \\ \Sigma_{\mathrm{v}} &= -2g_{0,2}\omega, \\ \Sigma_{\mathrm{d}}^{b} &= -2\big(d_{0,2}\Delta^b + d_{2,2}\sigma^2\Delta^b\big), \\ \Sigma_{\mathrm{d}}^{*b} &= -2\big(d_{0,2}\Delta^{*b} + d_{2,2}\sigma^2\Delta^{*b}\big), \\ U &= g_{2,0}\sigma^2 - g_{0,2}\omega^2 + d_{0,2}\Delta^{*b}\Delta^b + 3d_{2,2}\sigma^2\Delta^{*b}\Delta^b, \end{aligned} \tag{3}$$

and the auxiliary fields introduced are $\sigma = \langle\bar{q}q\rangle$, $\omega = \langle\bar{q}\gamma^0 q\rangle$, $\Delta^b = \langle i\bar{q}^c\varepsilon\epsilon^b\gamma_5 q\rangle$, and $\Delta^{*b} = \langle i\bar{q}\varepsilon\epsilon^b\gamma_5 q^c\rangle$.

The thermodynamical potential Ω of the system with finite temperature T and chemical potential μ is then obtained as

$$\begin{aligned}\Omega = {}& -2N_f V\bigg[\int\frac{d^3\mathbf{p}}{(2\pi)^3}E_{\mathbf{p}} \\ & + \frac{1}{\beta}\big\{\ln\big(1 + e^{-\beta E_{\mathbf{p}}^+}\big) + \ln\big(1 + e^{-\beta E_{\mathbf{p}}^-}\big)\big\} \\ & + \mathrm{sgn}\big(E_{\mathbf{p}}^-\big)E_\Delta^- + E_\Delta^+ \\ & + \frac{2}{\beta}\big\{\ln\big(1 + e^{-\mathrm{sgn}(E_{\mathbf{p}}^-)\beta E_\Delta^-}\big) + \ln\big(1 + e^{-\beta E_\Delta^+}\big)\big\}\bigg] \\ & + VU, \end{aligned} \tag{4}$$

where $\beta = 1/T$, $\tilde{\mu} = \mu + \Sigma_{\mathrm{v}}$, $M = m_0 + \Sigma_{\mathrm{s}}$, $E_{\mathbf{p}} = \sqrt{\mathbf{p}^2 + M^2}$, $E_{\mathbf{p}}^{\pm} = E_{\mathbf{p}} \pm \tilde{\mu}$, $E_\Delta^{\pm} = \sqrt{E_{\mathbf{p}}^{\pm 2} + |\Sigma_{\mathrm{d}}|^2}$, and $\mathrm{sgn}(E_{\mathbf{p}}^-)$ is the sign function. The corresponding scalar, vector, and scalar diquark densities, ρ_{s}, ρ_{v} and ρ_{d} are given by

$$\begin{aligned}\rho_{\mathrm{s}} = {}& -2N_f M\int\frac{d^3p}{(2\pi)^3}\frac{1}{E_{\mathbf{p}}}\bigg\{1 - n\big(E_{\mathbf{p}}^-\big) - n\big(E_{\mathbf{p}}^+\big) \\ & + \frac{E_{\mathbf{p}}^-}{E_\Delta^-}\tanh\frac{\beta E_\Delta^-}{2} + \frac{E_{\mathbf{p}}^+}{E_\Delta^+}\tanh\frac{\beta E_\Delta^+}{2}\bigg\}, \end{aligned} \tag{5}$$

$$\begin{aligned}\rho_{\mathrm{v}} = {}& 2N_f\int\frac{d^3p}{(2\pi)^3}\bigg\{n\big(E_{\mathbf{p}}^-\big) - n\big(E_{\mathbf{p}}^+\big) \\ & - \frac{E_{\mathbf{p}}^-}{E_\Delta^-}\tanh\frac{\beta E_\Delta^-}{2} + \frac{E_{\mathbf{p}}^+}{E_\Delta^+}\tanh\frac{\beta E_\Delta^+}{2}\bigg\}, \end{aligned} \tag{6}$$

$$\begin{aligned}\rho_{\mathrm{d}} = {}& -2N_f\Sigma_{\mathrm{d}}\int\frac{d^3p}{(2\pi)^3}\bigg\{\frac{1}{E_\Delta^-}\tanh\frac{\beta E_\Delta^-}{2} \\ & + \frac{1}{E_\Delta^+}\tanh\frac{\beta E_\Delta^+}{2}\bigg\}, \end{aligned} \tag{7}$$

where

$$\begin{aligned} n_q &= \frac{1}{1 + \exp\{\beta(E_p - \tilde{\mu})\}}, \\ n_{\bar{q}} &= \frac{1}{1 + \exp\{\beta(E_p + \tilde{\mu})\}}. \end{aligned} \tag{8}$$

The gap equation can be derived by minimizing the thermodynamical potential with respect to σ, ω, and Δ^*, their physical solutions then satisfy the stationary condition

$$\begin{pmatrix} \frac{\partial}{\partial\sigma}(\frac{\Omega}{V}) \\ \frac{\partial}{\partial\omega}(\frac{\Omega}{V}) \\ \frac{\partial}{\partial\Delta^*}(\frac{\Omega}{V}) \end{pmatrix} = \mathcal{G}\begin{pmatrix} \sigma - \rho_{\mathrm{s}} \\ \rho_{\mathrm{v}} - \omega \\ \Delta - \rho_{\mathrm{d}} \end{pmatrix} = \begin{pmatrix} 0 \\ 0 \\ 0 \end{pmatrix}, \tag{9}$$

where the effective couplings are

$$\mathcal{G} \equiv \begin{pmatrix} G_{s\sigma} & G_{v\sigma} & G_{d\sigma} \\ G_{s\omega} & G_{v\omega} & G_{d\omega} \\ G_{s\Delta} & G_{v\Delta} & G_{d\Delta} \end{pmatrix} \equiv \begin{pmatrix} -\frac{\partial \Sigma_s}{\partial \sigma} & -\frac{\partial \Sigma_v}{\partial \sigma} & -\frac{\partial \Sigma_d^*}{\partial \sigma} \\ -\frac{\partial \Sigma_s}{\partial \omega} & -\frac{\partial \Sigma_v}{\partial \omega} & -\frac{\partial \Sigma_d^*}{\partial \omega} \\ -\frac{\partial \Sigma_s}{\partial \Delta^*} & -\frac{\partial \Sigma_v}{\partial \Delta^*} & -\frac{\partial \Sigma_d^*}{\partial \Delta^*} \end{pmatrix} = \begin{pmatrix} 2(g_{2,0} + d_{2,2}|\Delta|^2) & 0 & 4d_{2,2}\sigma\Delta^* \\ 0 & 2g_{0,2} & 0 \\ 4d_{2,2}\sigma\Delta & 0 & 2(d_{0,2} + d_{2,2}\sigma^2) \end{pmatrix}. \quad (10)$$

When $\det(\mathcal{G}) \neq 0$, $\mathcal{G}$ has its inverse, and then the stationary condition leads to $\sigma = \rho_s$, $\omega = \rho_v$, and $\Delta = \rho_d$.

It has been shown that the effect of the ω^2 coupling on the phase diagram is suppressed by the nonlinear terms, $g_{4,0}\sigma^4$ and $g_{2,2}\sigma^2\omega^2$, in our previous paper [25]. Therefore, the vector coupling $g_{0,2}$ is fixed to the small value, $0.2g_{2,0}$. The adopted parameters for numerical calculations are summarized in Table 1. We examine both signs for $d_{2,2}$ since this is not determined within the model and they would lead to different physical pictures.

In the following, we discuss the phase diagrams obtained by adopting the models with the parameters summarized in Table 1 putting emphasis on the chiral–diquark coexistence at low-T. Fig. 1(a) graphs the phase diagram of the standard NJL model with the diquark condensate. The coexistence region is very small in this case. Blaschke et al. first pointed out the existence of this coexistence region adopting another parameter set without the ω^2 interaction [26]. Fig. 1(b) shows the effect of the ω^2 interaction, that is, it weakens both transitions and shifts the chiral restoration to the higher density side and consequently produces a coexistence phase at low-T. This confirms the result presented by Kitazawa et al. [17]. Comparison of Figs. 1(a) and 2(a) demonstrates the effect of the $\sigma^2\Delta^2$ coupling for the case of positive $d_{2,2}$. This nonlinear interaction shifts the CSC transition to lower density and consequently produces a coexistence phase. Fig. 2(b) includes both the ω^2 and the $\sigma^2\Delta^2$ interactions. They coherently add up in this case. This result can be understood from the expressions of the effective couplings that lead to

$$\Sigma_s = -G_{s\sigma}\sigma = -2\big(g_{2,0} + d_{2,2}|\Delta|^2\big)\sigma \quad (11)$$

and

$$\Sigma_d = -G_{d\Delta}\Delta = -2\big(d_{0,2} + d_{2,2}\sigma^2\big)\Delta, \quad (12)$$

in which the former indicates that positive $d_{2,2}$ enhances $|\Sigma_s|$ when $\Delta \neq 0$ exists and the latter indicates that positive $d_{2,2}$ enhances $|\Sigma_d|$ when $\sigma \neq 0$ exists. This means that the $\sigma^2\Delta^2$ interaction acts only when the ω^2 interaction makes σ and Δ coexisting. Figs. 3(a) and 3(b) graph the result of the negative $d_{2,2}$. In this case the ω^2 interaction and the $\sigma^2\Delta^2$ one are destructive to each other and consequently the coexistence region becomes very small.

As mentioned above, the sign and the magnitude of the eight-quark interaction is not determined within the present model. The positive $d_{2,2}$ results in a large coexistence region. The sign is supported by the result of the quark–diquark model for the nucleon [19] that the diquark interaction is sizably stronger in the normal baryon-number density region than in the high density one. However, further analysis is needed to determine the strength of the coupling more precisely in the normal density region. Oppositely, if the negative sign is favored by some reason, the coexistence region shrinks and the two phase transitions occur at almost the same T and μ. In the vicinity,

Table 1
Summary of the parameter sets. The coupling constants are shown in GeV^{-2}. For all cases we adopt $m_0 = 0.0055$ GeV, $\Lambda = 0.6315$ GeV, and $\sigma_0 = -0.03023\ \mathrm{GeV}^3$. Here, G_ω and G_Δ are $0.2g_{2,0}$ and $0.6g_{2,0}$, respectively. (See Table 1 in Ref. [25] for comparison.)

Model	$g_{2,0}$	$g_{0,2}$	$d_{0,2}$	$\lvert d_{2,2}\rvert\sigma_0^2$
NJL + Δ^2	5.498	0	G_Δ	0
NJL + $\omega^2 + \Delta^2$	5.498	G_ω	G_Δ	0
NJL + $\Delta^2 + \sigma^2\Delta^2$	5.498	0	G_Δ	$0.2G_\Delta$
NJL + $\omega^2 + \Delta^2 + \sigma^2\Delta^2$	5.498	G_ω	G_Δ	$0.2G_\Delta$

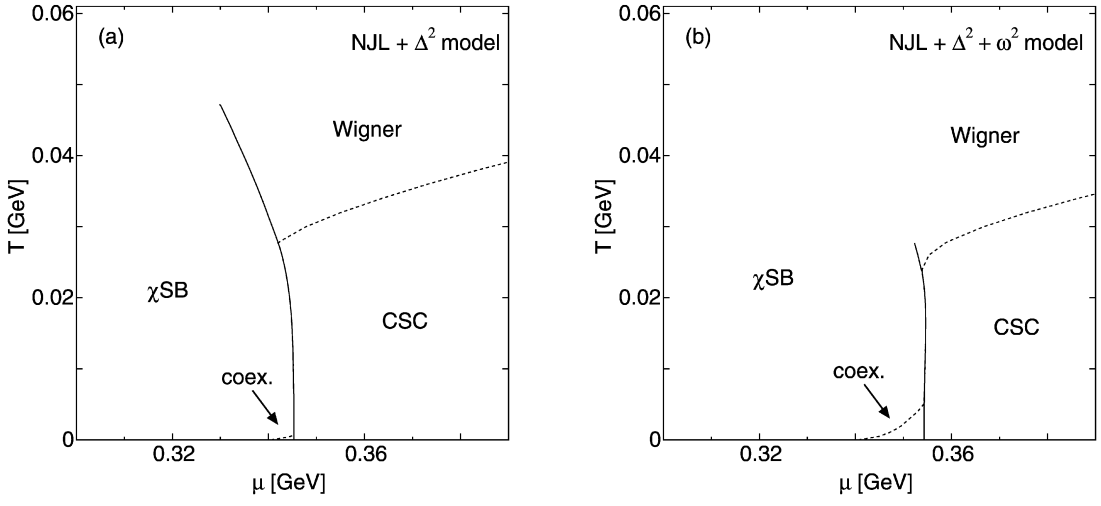

Fig. 1. Phase diagrams given by (a) the standard linear NJL model and (b) the extended NJL model that includes the ω^2 interaction.

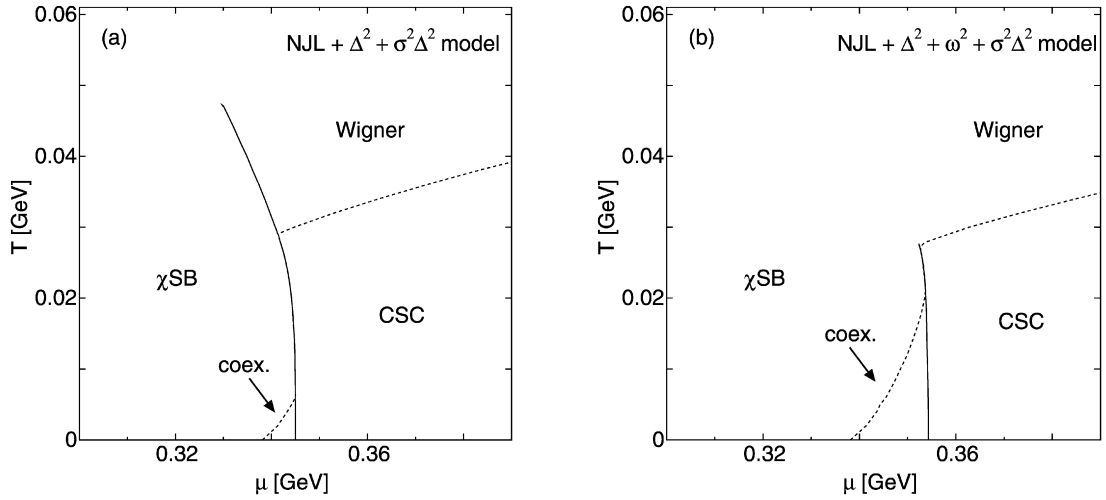

Fig. 2. Phase diagrams given by (a) the extended NJL model that includes the $\sigma^2\Delta^2$ interaction and (b) that includes the ω^2 and the $\sigma^2\Delta^2$ interactions. In these calculations $d_{2,2}$ is positive.

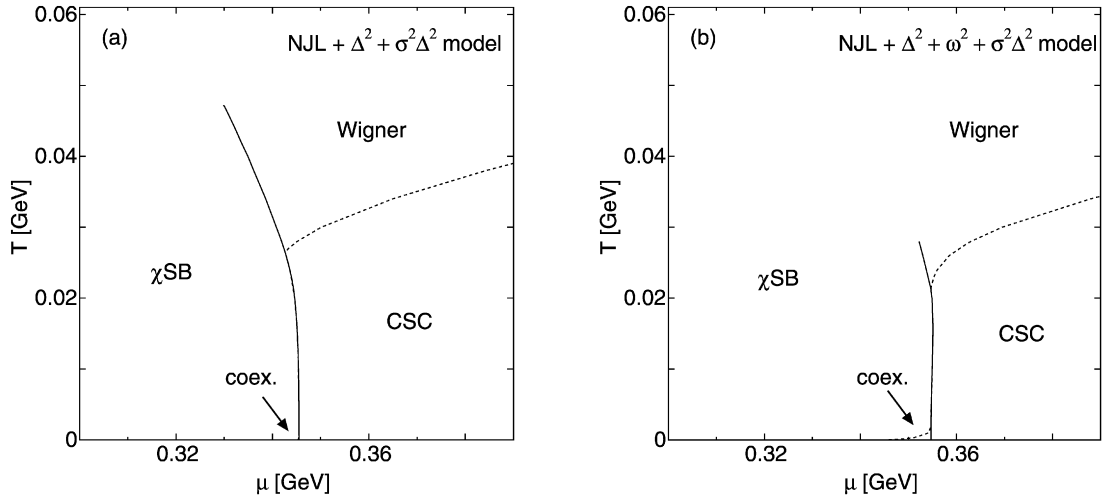

Fig. 3. The same as Fig. 2 but $d_{2,2}$ is negative.

the order parameters, σ and Δ, are small. Such a region is an ideal playground for the GL approach, since the free energy is expanded with respect to them. In other words, when the sign is positive, the GL model is not useful to determine the phase diagram except for the high-T region where both the order parameters are small.

We have studied the interplay of the chiral and the color superconducting phase transition in an extended Nambu–Jona-Lasinio model with a multi-quark interaction that produces the nonlinear $\sigma^2\Delta^2$ coupling. We have found that the size of the chiral–diquark coexistence region is sensitive to the sign of the coupling. The positive sign is supported by the quark–diquark model for the nucleon, but further analysis is needed to determine the density dependence of the diquark interaction more precisely. Meanwhile, the negative sign is the prerequisite for the applicability of the Ginzburg–Landau approach that has already been applied to determine the phase diagram. Thus, the determination of the sign is an important subject related to the phase diagram.

References

[1] T.D. Lee, Nucl. Phys. A 750 (2005) 1.
[2] M. Gyulassy, L. McLerran, Nucl. Phys. A 750 (2005) 30.
[3] E.V. Shuryak, Nucl. Phys. A 750 (2005) 64.
[4] K. Rajagopal, F. Wilczek, Handbook of QCD, vol. 3, World Scientific, Singapore, 2000.
[5] Y. Nambu, G. Jona-Lasinio, Phys. Rev. 122 (1961) 345.
[6] Y. Nambu, G. Jona-Lasinio, Phys. Rev. 124 (1961) 246.
[7] S.P. Klevansky, Rev. Mod. Phys. 64 (1992) 649.
[8] T. Hatsuda, T. Kunihiro, Phys. Rep. 247 (1994) 221.
[9] M.A. Stephanov, Phys. Rev. Lett. 76 (1996) 4472.
[10] M.A. Halasz, A.D. Jackson, J.J.M. Verbaarschot, Phys. Lett. B 395 (1997) 293.
[11] P.N. Meisinger, M.C. Ogilvie, Phys. Lett. B 379 (1996) 163.
[12] K. Fukushima, Phys. Lett. B 591 (2004) 277.
[13] C. Ratti, M.A. Thaler, W. Weise, Phys. Rev. D 73 (2006) 014019.
[14] S.K. Ghosh, T.K. Mukherjee, M.G. Mustafa, R. Ray, Phys. Rev. D 73 (2006) 114007.
[15] T. Sakaguchi, K. Kashiwa, M. Matsuzaki, H. Kouno, M. Yahiro, Contr. Eur. J. Phys., in press.
[16] M. Buballa, Nucl. Phys. A 611 (1996) 393.

[17] M. Kitazawa, T. Koide, T. Kunihiro, Y. Nemoto, Prog. Theor. Phys. 108 (2002) 929.
[18] J. Berges, K. Rajagopal, Nucl. Phys. B 538 (1999) 215.
[19] S. Lawley, W. Bentz, A.W. Thomas, Phys. Lett. B 632 (2006) 495.
[20] T. Hatsuda, M. Tachibana, N. Yamamoto, G. Baym, Phys. Rev. Lett. 97 (2006) 122001.
[21] A.A. Osipov, B. Hiller, J. da Providência, Phys. Lett. B 634 (2006) 48.
[22] A.A. Osipov, B. Hiller, J. Moreira, A.H. Blin, J. da Providência, Phys. Lett. B 646 (2007) 91.
[23] R. Huguet, J.C. Caillon, J. Labarsouque, Nucl. Phys. A 781 (2007) 448.
[24] R. Huguet, J.C. Caillon, J. Labarsouque, Phys. Rev. C 75 (2007) 048201.
[25] K. Kashiwa, H. Kouno, T. Sakaguchi, M. Matsuzaki, M. Yahiro, Phys. Lett. B 647 (2007) 446.
[26] D. Blaschke, M.K. Volkov, V.L. Yudichev, Eur. Phys. J. A 17 (2003) 103.